Development and Testing of a GIS-Based Method to Detect and Characterize Sinkholes

A Thesis Presented for the

Master of Science

Degree

The University of Tennessee, Knoxville

Bridgette Ingram Fritz

May 2020

ACKNOWLEDGEMENTS

This journey would not have been possible without the support of my family, friends, mentors, and professors who guided and encouraged me along the way. I would like to first extend a huge thank you to my mom and dad for their unwavering love and support. I appreciate you more than words can say, and I love you twice as much. I would also like to express my sincerest gratitude to my sister for always being the voice on the other end of the phone when I most needed it. In the words of Dad "You're my hero, Sis." I would be remiss if I didn't acknowledge my editor-in-chief Ember Lundy. Your constant and overwhelming support and encouragement kept me going. Of course, thank you to the friends I met along the way, Njoroge Gathango, Sandhya Nepal, Adam Aslamadisi, Dani Dami, Danny Burrow, Jacob Cecil, Brooke Rose, Paula Perilla, and many others. Our shared love and laughter will carry well beyond the walls of Burchfiel Geography, and for that I am very grateful. And to my committee Dr. Liem Tran, Dr. Sally Horn, and Dr. Larry McKay, thank you for your guidance and support through the development of this thesis. Finally, I would like to thank my funding sources for without them this thesis would have not been possible. Major funding was provided by the University of Tennessee, College of Arts and Sciences, and the Donald and Florence Jones Geohydrology Endowment at the University of Tennessee. Additional support was provided by a grant to Drs. Larry McKay, Sally Horn, and Liem Tran from the Electric Power Research Institute (EPRI Agreement: 00-10005236), and by the Department of Geography.

ABSTRACT

With the development of modern remote-sensing technology, high-resolution remotely sensed data can be used to provide more accurate mapping and analyses of surface terrain including sinkholes. The focus of this thesis is on developing a method for detecting and characterizing sinkholes including identifying particular sinkholes with the potential of having preserved paleoflood evidence. The proposed method is applied to the case study area within the Upper Tennessee River Basin, Knox County, Tennessee. The results of the method identified 7,248 likely sinkholes within the county. Based on the accuracy assessment, with a true positive rate of 84%, the results of the case study suggest that this method can be used to identify sinkholes in karst regions. Not only can the method be used to successfully identify sinkholes, but it also has several strengths in terms of sinkhole detection compared to traditional methods that rely on outdated topographic maps, aerial imagery, and field observations.

TABLE OF CONTENTS

Chapter One: Introduction, Objectives, and Background 1
Research Objectives 1
Sinkhole Overview 1
Sinkholes in Tennessee 2
Sinkholes in Knox County, Tennessee 3
Traditional methods of Sinkhole Detection 3
Paleoflood Research Overview 4
Sinkholes as Recorders of Past Floods 5
Tennessee River Paleoflood Research 5
Flood History of Knox County 6
Case Study Overview 7
Chapter Two: Methods 9
Method Overview 9
Case Study Area 12
Case Study in Detail 13
Step One: Delineate Depressions Using the Level-Set Method and Derive Their Morphometric Characteristics 13
Step Two: Develop a Training Sinkhole Dataset 14
Step Three: Identify Likely Sinkholes 14
Step Four: Conduct an Accuracy Assessment 15
Step Five: Identify likely sinkholes with the potential for the preservation of paleoflood evidence 16
Chapter Three: Results and Discussion 22
Results 22
Step One: Delineate Depressions 22
Step Two: Develop a Training Sinkhole Dataset 22
Step Three: Identify Likely Sinkholes 23
Step Four: Conduct an Accuracy Assessment 23

Step Five: Identify likely sinkholes with the potential for the preservation of paleoflood evidence 24
Discussion 24
Chapter Four: Conclusions 35
List of References 37
Vita 44

LIST OF TABLES

Table 2.1. List of Data Used and Their Source..... 17
Table 3.1. Summary Statistics of Depressions..... 32
Table 3.2. Summary Statistics of Training Sinkhole Depressions..... 32
Table 3.3. Accuracy Assessment for Identified Sinkholes 34

LIST OF FIGURES

Figure 2.1. Map of Case Study Area: Knox County, Tennessee 18
Figure 2.2. Generalized Geologic Map of Tennessee 19
Figure 2.4. Example of FEMA Flood Hazard Extent Along the Tennessee River in Knox County, Tennessee 20
Figure 3.1. Depressions in Knox County, Tennessee 30
Figure 3.2. Examples of Elongation Values 31
Figure 3.3. Examples of Complexity Values 31
Figure 3.4. Overlapping Density Plots of Depressions and Training Sinkholes 33

CHAPTER ONE
INTRODUCTION, OBJECTIVES, AND BACKGROUND

This thesis work is part of a larger project studying the paleoflood history of the Upper Tennessee River Basin. In this chapter I first lay out the research objectives. I then provide an overview of sinkholes. Next, I briefly describe sinkhole detection methods. Then I discuss paleoflood research including how sinkholes can serve as recorders of past floods and the paleoflood research that is being conducted along the Tennessee River. Finally, I end this chapter by providing an overview of the case study in Knox County, Tennessee that I conducted to test the method that I developed.

Research Objectives

The objectives of this thesis are as follows:

I. To develop a method to detect and characterize sinkholes using ArcGIS,
II. To extend the method to identify examples of sinkholes with the potential of having preserved paleoflood evidence, and
III. To apply this method to create an enhanced sinkhole inventory for a karst-rich case study area (Knox County) within the Upper Tennessee River Basin and identify sites that have the potential to preserve ancient flood deposits.

Sinkhole Overview

The term karst is used to describe regions of highly soluble and porous rock including carbonate rocks such as limestone, gypsum, and dolomite. Because limestone is one of the most widespread sedimentary rocks and is largely responsible for the development of karst features, karst landscapes and features (including sinkholes) can be found worldwide (Waltham, Bell, & Culshaw, 2005). In the United States, 48 of the 50 states have karst regions (Kuniansky, Weary, & Kaufmann, 2015). Carbonate-rock aquifers and solution features such as caves and sinkholes are common in regions with this geological composition (Galloway, Jones, & Ingebritsen, 2000; Hampson, Treece, Johnson, Ahlstedt, & Connell, 2000). Although sinkholes are typically circular, sub-circular, or elliptical in shape, their depths and diameters can vary greatly from fractions of a meter to kilometers (Angel, Nelson, & Panno, 2004; Bondesan, Meneghel, &

Sauro, 1992; Jennings, 1971; Jones & White, 2012; Ju, Young, Chul, & Chang, 2016). This variation results in diverse forms from dish and bowl-shaped features to conical and cylindrical features (Jennings, 1971; Theilen-Willige, Malek, Charif, El Bchari, & Chaïbi, 2014). While the greatest sinkhole-related damages occur in the seven states of Florida, Texas, Alabama, Missouri, Kentucky, Pennsylvania, and Tennessee, there is the potential for sinkhole development across the United States (Kuniansky et al., 2015; Thornbush, 2017). Tennessee is a site of particular interest for sinkhole research as two-thirds of the state is covered by karst landscapes (Moore & Drumm, 2018).

Sinkholes in Tennessee

Despite being a region with a high density of karst features, very little information is recorded on sinkholes in Tennessee. In 1977, Miller produced a karst hazards map for the state. This map depicted "karst areas" and "areas with a high density of karst features" based on geological observations and analysis of topographic maps and ground observations (Miller & Sitterly, 1977). In addition, The Tennessee Geological Survey (TGS) has published a document that includes information on sinkholes in eastern Tennessee (Kohl, 2001). The TGS also funded a report for Montgomery County that outlines criteria to identify sinkholes that are likely to collapse (Kemmerley, 1980). In a 2001 article, Shofner, Mills, & Duke created sinkhole index maps for the state of Tennessee using the state's United States Geological Survey (USGS) 7.5-minute quadrangles (Shofner, Mills, & Duke, 2001).

Building upon the work of Shofner, Mills, & Duke (2001), Dunigan (2019) recorded the latitude and longitude of hachured contours visible on the state's USGS 7.5-minute quadrangles using online topographic maps to uncover more than 54,000 sinkholes in the state of Tennessee. As of November 29, 2019, this information is available on the Tennessee Landforms website that Dunigan maintains (Dunigan, 2019). Also available on the Tennessee Landforms website are Chuck Sutherland's sinkhole identification results gathered using ArcMap software and spatial analysis. Sutherland identified probable sinkholes with a depth of at least 3 meters using the state's 10-meter DEMs and listed their location, area, perimeter, depth, and volume. The raw data included 21,365 depressions (identified as probable sinkholes) with a depth of at least 3 meters; however, Sutherland found that at least 15.4% of these probable sinkholes were false sinkholes (depressions incorrectly classified as sinkholes), and he reported in his last update that

scrubbing is still ongoing (Dunigan, 2019). In the 2001 study by Shofner, Mills, & Duke, Knox County was identified as an area in Tennessee with highly developed karst (Shofner et al., 2001).

Sinkholes in Knox County, Tennessee

Harris (1973) published a map for Knox County that delineated areas with abundant sinkholes. He found that sinkholes in the county varied from a few conical steep-sided sinkholes to numerous broad and nearly flat-bottomed sinkholes. In addition, Harris noted that the conical sinkholes are typically less than a few hundred feet in diameter and could be as great as 100 feet deep. By comparison, flat-bottomed sinkholes are typically a few hundred to several thousand feet in diameter and could be as little as a few feet deep (Harris, 1973) In 1987 researchers at Oak Ridge National Laboratory (ORNL) inventoried sinkhole activity in the Valley and Ridge Province of East Tennessee that encompasses Knox County. For this inventory researchers focused on recording the development of recent sinkholes in order to support ongoing studies researching the environmental impact of waste disposal in karst settings. This inventory was produced by reviewing the available literature and by conducting phone interviews with the various federal, state, and county agencies that were expected to have information on recent sinkhole development (Ketelle, Newton, & Lamoreaux, 1987; Newton & Tanner, 1987). Researchers identified 256 cases of recent sinkhole subsidence, 16 of which occurred in Knox County (Newton & Tanner, 1987). In 2013, the Tennessee Department of Transportation (TDOT) created a karst map for a portion of south Knox County in preparation for a potential roadway project. This map identified numerous sinkholes, including a series of very large sinkholes that were multiple hectares in area (Moore, 2013). The Tennessee Landforms website currently contains information on the 1,663 likely sinkhole depressions in Knox County, 697 of which had a depth of at least 3 meters (Dunigan, 2019).

Traditional methods of Sinkhole Detection

With the exception of Sutherland's 2013 research, the information that exists on sinkholes in Knox County was developed using traditional methods of sinkhole detection that depend primarily on field observation, interpretation of aerial imagery, and visual analysis of topographic maps. These methods often result in sinkhole inventories that are inaccurate and incomplete for several reasons (Denton, Hogan, & Thomas, 2016; Gutiérrez et al., 2011; Zhu,

Taylor, Currens, & Crawford, 2015). For example, while large sinkholes are often recorded in inventories based on analysis of topographic maps, small sinkholes are often missing. In other words, sinkholes that are large enough to be represented on USGS topographic maps (with contour intervals ranging from 10 feet or less in relatively flat areas to intervals of 100 feet or more in mountainous regions) are accurately represented in sinkhole inventories developed from topographic maps (US Geological Survey, 1993; Zhu et al., 2015). However, relatively shallow sinkholes that have a depth less than the contour interval are not represented on topographic maps and therefore are not recorded on sinkhole inventories developed solely from analysis of topographic maps. Additionally, sinkholes are highly dynamic with the potential of developing or being filled at any time. Therefore, even the most recent USGS topographic maps (developed more than 25 years ago) are often outdated in terms of accurate sinkhole locations (Brinkman 2013; Zhu 2015). Another shortcoming is that researchers using these methods often consider all hachured contours on topographic maps to represent sinkholes and do not include additional information on sinkhole characteristics to filter and eliminate non-sinkhole depressions.

Modern remote-sensing technology provides high-resolution data that can be used to accurately map and analyze surface terrain, including sinkholes. Thus, these data can be used to develop updated and enhanced sinkhole inventories for karst regions worldwide (Denton et al., 2016; Launspach, 2013; Theilen-Willige et al., 2014; Wu, Deng, & Chen, 2016). These improved sinkhole inventories can serve important purposes including use in flood-hazard mapping, land-use planning, sinkhole-hazard mapping, and paleoenvironmental reconstructions.

Paleoflood Research Overview

The study of paleofloods gives researchers insight into the frequency and magnitude of past floods to extend our knowledge of historical flood events for regions with a scarcity of historical flood records (Benito & Diez-Herrero, 2015; Benito & Thorndycraft, 2004; Oliva et al., 2016; Pickup, Marks, & Bourke, 2002). Researchers can better understand and reconstruct paleoflood histories by incorporating multiple lines of evidence preserved in historical, geomorphological, stratigraphic, and biological records. Historical evidence of past floods can include written, oral, or photographic records of the events (Bauer, 2010; Benito & Thorndycraft, 2004). Geomorphological evidence of past floods can include erosional and depositional features that indicate flooding (Stewart & LaMarche, 1967). Stratigraphic evidence of past floods can

include abrupt changes in grain size, sediment color and composition, and presence of intercalated deposits of different origin (House, 1991; Wilhelm et al., 2013). Biological evidence of past floods can include histories preserved in the annual growth rings and irregular growth patterns of trees in the affected areas, as well as changes in relative pollen assemblages, relative macroinvertebrate assemblages, and relative diatom ratios to name a few (George, 2010; Thorndycraft, Hu, Oldfield, Crooks, & Appleby, 1998; Tongwen, Yujiang, Feng, & Shulong, 2018; Wiklund, Bozinovski, Hall, & Wolfe, 2010). Researchers search for such evidence to reconstruct paleoflood histories.

Sinkholes as Recorders of Past Floods

The assessment of past flood events depends on a continuous record of sediment during the observed period; therefore, analysis of sediment cores collected from sinkholes offers an advantage for reconstructing long-term flood histories in comparison to analysis of slackwater deposits collected from broad overbank areas (Gutiérrez et al., 2017). For example, evidence in slackwater deposits on broad overbank areas may be lost due to erosion from subsequent flood events or biological activity. However, as closed topographic depressions, sinkholes can serve as superior collection sites due to their ability to trap and maintain flood evidence preserved in sediments (Crownover, Collins, & Lietzke, 1994; Gutiérrez et al., 2017; Turnage, Lee, Kim, & Larse, 1997). In that context, researchers consider floodplain sinkholes as promising locations to collect sediment cores that contain proxy indicators of paleofloods.

Tennessee River Paleoflood Research

Paleoflood studies have been successfully undertaken in the western part of the United States where the more arid and rocky conditions are well-suited to preserve evidence of past floods. However, in the southeastern United States where few gauging stations have record lengths in excess of 100 years, long-term flood histories are widely unknown (Davis, 2017; Wang & Leigh, 2012). Paleoflood research has been a topic of increasing interest following the 2011 meltdown at the Fukushima Daiichi Nuclear Power Plant in Japan after a catastrophic flood event. The Tennessee Valley Authority (TVA) and the Electrical Power Research Institute (EPRI) are now working to understand whether sufficient proxy indicators exist in the southeastern part of the United States despite the presence of a humid climate and wetter soils

that are more likely to erode such evidence (Davis, 2017). My thesis research is part of a joint effort to understand paleoflood histories along the Tennessee River and is composed of researchers from the USGS and several regional universities including the University of Georgia, the University of Alabama, the University of Tennessee, Murray State University, and Baylor University.

Flood History of Knox County

Though records of the Tennessee River stages at Knoxville have been maintained periodically since 1883, continuous records began in 1899. In addition to the gauge records, accounts of large floods have been collected from local newspapers and reports by TVA engineers. With a gauge height of 45 feet, the largest flood of record for Knox County occurred on March 10, 1867. Other great floods in order of magnitude were those of February 26, 1875 (43.2 feet), March 1, 1902 (34.4 feet), May 23, 1901 (33.1 feet), April 2, 1896 (32.0 feet), July 18, 1916 (31.7 feet), April 1, 1886 (31.0 feet), and March 5, 1917 (31.0 feet) (Tennessee Valley Authority, 1958). The TVA's Flood Control Branch estimated the gauge heights for the floods that occurred prior to 1900 while the USGS determined the gauge heights of the floods that occurred after 1900. Other great floods are documented in the years of 1791, 1797, 1821, 1826, and 1847, although the gauge heights for these floods are unknown (Tennessee Valley Authority, 1958). In the 1940s, dams were built in the river basin as part of a comprehensive plan to provide electricity and flood control in the Tennessee Valley (Tennessee Valley Authority, 1961, 2019). Built in 1941 and 1943 respectively, the Cherokee and Douglas Dams help regulate floods on the Holston and French Broad Rivers upstream from Knoxville (Tennessee Valley Authority, 1961). No significant flood has occurred in Knox County since the development of these dams; however, in February 1957 a major flood would have likely occurred if not for the regulation provided by the Cherokee and Douglas Dams. It should be noted that the 1867 flood is projected to have been 18 feet lower if it had been regulated by current dams (Tennessee Valley Authority, 1958). Although regulation can reduce flooding, large floods are possible in Knoxville even with the regulation provided by storage reservoirs. It is particularly important to understand the paleoflood history along the Tennessee River as the region is home to several nuclear power plants (including Watts Bar, Sequoyah, and Browns Ferry). The geology and physiography of this region render these plants vulnerable to flooding. Paleoflood studies conducted in this region

can help researchers understand the potential flood risk for these vulnerable sites (Harden & O'Conner, 2017).

Case Study Overview

I selected Knox County, Tennessee as a case study area within the Upper Tennessee River Basin to test the method that I developed. Although Knox County is a region with a high density of sinkholes, there are few records on sinkhole locations and characteristics in the county. In addition, much of the information that exists is based on traditional methods of sinkhole detection that rely on outdated topographic maps and field observations that cover relatively small or disjunct study areas. Furthermore, sinkhole inventories developed from visual analyses of topographic maps often consider all hachured contours to represent true sinkholes (depressions correctly classified as sinkholes) and do not include additional information on sinkhole characteristics that can be used to filter out non-sinkhole depressions. The method I developed consists of two main components: 1) to detect and characterize sinkholes and 2) to identify sinkholes with the potential of having preserved paleoflood evidence. For this thesis, I applied the level-set method developed by Wu et al. (2018) to detect surface depressions in Knox County. The level-set method is composed of four steps: 1) filtering to smooth DEMs; 2) extracting depressions based on the priority flood algorithm; 3) delineating nested depressions and; 4) characterizing the hierarchy of nested depressions (Wu et al., 2018). After I derived surface depressions in the study area, I applied hard and soft filters to limit the results to the depressions that are most likely to represent sinkholes. Hard filters were based on the morphometric characteristics of a set of verified sinkholes in the study area. These sinkholes were verified through analyses of topographic maps and aerial imagery. Soft filters were applied to flag identified sinkholes for two reasons: 1) to identify sinkholes in close proximity to man-made structures and 2) to identify sinkholes that could be suitable paleoflood sampling sites. Through this work, I produced an enhanced sinkhole inventory for Knox County. This inventory was then used to identify sinkholes within the 100- and 500-year floodplain of the Tennessee River based on flood zone designations regulated by the Federal Emergency Management Agency (FEMA). Because I was interested in finding sinkholes in which I could study paleoflood deposits together with environmental proxies preserved in sediments, I identified

sinkholes that coincided with wetlands that are recorded in the US Fish and Wildlife Service wetland database.

CHAPTER TWO
METHODS

Method Overview

In this section of the thesis, I will outline the steps used to develop a method for detecting and characterizing sinkholes as well as how the results of the method can be used to identify particular sinkholes with the potential of having preserved paleoflood evidence. The steps of the method are as follows: 1) delineate depressions using the level-set method and derive their morphometric characteristics; 2) develop a training sinkhole dataset; 3) identify likely sinkholes; 4) conduct an accuracy assessment**;** and 5) identify likely sinkholes with the potential of having preserved evidence of paleofloods (see Figures 2.4.-2.6.).

The first step of the method involves applying the level-set method developed by Wu et. al (2018) to detect surface depressions across the landscape with the basic assumption that sinkholes are a subset of all depressions(Wu et al., 2016, 2018). This algorithm requires three parameters to be predetermined: minimum size of depressions, minimum depth, and slicing interval (Wu et al., 2018). The morphometric characteristics then must be derived in order to separate sinkholes from other non-sinkhole depressions in step three. Morphometric characteristics including area, depth, shape complexity, elongation, slope, and curvature must be calculated for each of the derived depression polygons. Details are as follows:

Area

Area in square meters is calculated using the ArcGIS *calculate geometry* tool in the ESRI ArcGIS geoprocessing toolbox.

Depth

Depth in meters is calculated by first using the *zonal statistics* tool in the spatial analyst toolbox to derive the maximum and minimum elevation for each depression polygon and then subtracting the minimum elevation from the maximum elevation.

Shape Complexity

Shape complexity is calculated using the *complexity* tool available through the open-source GIS software package WhiteboxTools (Lindsay, 2016). Shape complexity (unitless) measures the overall irregularity of the depression polygons and serves as a parameter for

assessing the complexity of a polygon that is independent of its elongation. The formula for shape complexity is as follows:

$$SCI = 1 - A / Ah$$

where A is the polygon's area and Ah is the area of the convex hull containing the polygon.

Elongation Ratio

The elongation ratio is calculated using the *elongation* tool also available through the open-source GIS software package WhiteboxTools (Lindsay, 2016). Elongation (unitless) measures the circularity versus linearity of a given depression and its formula is as follows:

$$E = 1 - S / L$$

Where S is the short-axis length, and L is the long-axis length. Axes lengths are determined by the minimum bounding box.

Slope

To derive slope for the walls of the depression the analyst must first delineate polygons of the walls of the depressions.

This process involves four steps:

1) Use the *select by location* tool to select all 2-foot contours that intersect the depression's polygons;

2) Select the minimum contour within each depression;

3) Convert the contour line to a polygon using the *polyline to polygon* tool; and

4) Subtract the base contour polygon from the depression polygon using the *erase* tool, resulting in polygons of the walls of the depression.

Slope in percent must then be generated for the walls of the depressions using the *slope* tool in the 3D Analyst toolbox. Then by applying the *zonal statistics* tool one can derive the mean slope for the walls of each depression.

Curvature

To derive curvature for the walls of the depressions, the analyst must use the same polygons of the walls of the depressions used for calculating slope. Curvature in meters can then be generated for walls of depression using the *curvature* tool in the 3D Analyst toolbox.

Combining the level-one depressions that I identified with the aforementioned morphometric characteristics results in a dataset that includes the location and morphometric properties of all depressions derived in the study area.

The second step of the method is to develop a training sinkhole dataset. The purpose of the training sinkhole dataset is to serve as a basis for separating true sinkholes from other non-sinkhole depressions based on the morphometric characteristics of verified sinkholes. The training sinkhole dataset should include a set of verified sinkholes within the study area. For regions where there exists a sinkhole dataset, the analyst should verify the recorded sinkholes based on coincidence with karst regions as well as presence on topographic maps (although recently developed sinkholes may not be recorded on topographic maps) and aerial imagery. For regions without previously recorded sinkhole information, field observations will be required to derive a set of verified sinkholes to serve as training data.

The third step of the method is to apply a two-step filtering process to identify the depressions that are most likely to represent true sinkholes. First, the analyst should use the morphometric characteristics of training sinkholes to identify likely sinkholes. Then, because urban and agricultural development could create false positives that resemble true sinkholes in terms of morphometric properties, the analyst should conduct additional analyses to flag these locations for further validation. Therefore, in the second step of the filtering process, the analyst should apply soft filters through the use of buffers and intersect analysis to flag these potential false positives for review. To identify potential non-sinkhole depressions that could be the result of urban development, buffers should be applied to building footprint shapefiles and roads shapefiles. For roads shapefiles, the analyst should consider the road type when creating the buffer; for example, an alley would have a smaller buffer than a major arterial road.

In addition to anthropogenic features, sinkholes that coincide with wetlands and intersect soils of fluvial origin should be flagged as these locations are potentially suitable for paleoflood sampling. Identifying sinkholes that intersect wetland locations is not only important for identifying potential paleolimnological sampling sites but is also important for flagging potential falsely identified sinkholes that could be farm ponds, retention ponds, or other anthropogenic water features. To flag the sinkholes of interest (those that intersect building and road buffers, wetlands, or soils of fluvial origins), a new column should be created in the attribute table and

the *select by attribute* tool should be used to select the sinkholes that intersect these features. Next, the intersecting sinkholes should be flagged by using the *field calculator* tool to assign the value of one to intersecting sinkholes and zero to non-intersecting sinkholes.

The fourth step of the method is to conduct an accuracy assessment. First, the analyst must identify a set of verified sinkholes and non-sinkhole depressions to serve as sample data for the assessment. To do so, the create *random points* tool is used to identify the sinkhole and non-sinkhole locations at random. This is accomplished by buffering the random points to create focus areas in which sinkholes and non-sinkhole depressions are identified. In the buffered region, the analyst should identify a set of verified sinkholes and non-sinkhole depressions based on visual analysis of aerial imagery and high-resolution contour data where applicable. High-resolution contour data provide an advantage over visual analysis alone because contour data allow the analyst to identify some sinkholes that would otherwise be difficult to identify (e.g., sinkholes that are relatively shallow or that fall within an area of dense canopy cover). Next, a contingency table should be developed to test the sample data against the results of the method.

The fifth step of the method is to identify sinkholes with the potential for the preservation of paleoflood evidence. First, the analyst should intersect the sinkholes with recorded flood zones to identify sinkholes within the floodplain. The next step is to identify if the sinkhole is old enough to potentially record paleoflood records based on its presence on historical topographic maps. The USGS historical topographic maps collection is a valuable resource to identify if a potential floodplain sinkhole is old enough to preserve paleoflood evidence. The method outlined above was applied in a case study that will be discussed in detail in the following sections.

Case Study Area

The case study area of this research is Knox County, Tennessee. Knox County (Figure 2.1.) is in the Great Valley of East Tennessee with the Cumberland Plateau to the west and the Great Smoky Mountains to the east (National Park Service, 2019). This valley is part of a subrange of the Appalachian Mountains known as the Valley and Ridge physiographic province (National Park Service, 2019). The province is characterized by early Paleozoic sedimentary rocks including limestone, shale, dolomite, and sandstones (Hampson et al., 2000; Luther, 2017; Rodgers, 1953; Swingle, 1965) (Figure 3.2.). Common in this province are carbonate rock aquifers and features typical of karst landscape, such as sinking streams, caves, and sinkholes

(Moore & Drumm, 2018). Formed by the confluence of the Holston and French Broad Rivers in east Knox County, the Tennessee River is a prominent feature of the region. Data used in this study include LIDAR DEMs, locations of recorded sinkholes from a previous study, karst areas in shapefile format, two-foot contours (shapefiles), roads (shapefiles), building footprints (shapefiles), wetland locations (shapefiles), and historical topographic maps. Table 2.1 displays a complete list of the data and their sources.

Case Study in Detail

Step One: Delineate Depressions Using the Level-Set Method and Derive Their Morphometric Characteristics

I applied the level-set method developed by Wu et al. (2018) to detect depressions across Knox County. For the required parameters, I chose a minimum depression size of 45 square meters and a minimum depth of 0.3 meters based on visual observation of recorded sinkholes and the limited existing information on recorded sinkholes in the region. 45 square meters is smaller than most previously recorded sinkholes in the region based on results from a preliminary analysis**;** however, I wanted to select a value below that of existing sinkholes records to allow for the identification of small sinkholes that were previously undetected. In addition, the depth threshold of 0.3 meters is shallower than previously recorded sinkholes in the region. I found that the lower range of depth values for previously recorded sinkholes in the region was approximately 1 meter; however, I selected a depth value of 0.3 meters as this value is between the lower range of previously recorded sinkhole depth values and the DEM vertical accuracy of ca 18.5 cm. The selection of this value could allow for the identification of sinkholes that were previously undetected. Based on the recommendation for the slicing interval to be two to three times the DEM vertical accuracy, I set the slicing interval at 0.3 meters (Wu et al., 2018). Further analyses focus on level-one depressions (referred to simply as depressions hereafter) as all higher-level depressions are formed by the merging of level-one depressions. For example, the merging of two level-one depressions results in a level-two depression, whereas the merging of a level-one depression and a level-two depression results in a level-three depression (Wu et al., 2018). Therefore, as level-one depressions are the building-block of all higher-level depressions, focusing on level-one depressions is considered sufficient for identifying likely sinkholes within the region.

Step Two: Develop a Training Sinkhole Dataset

To identify depressions that could serve as training sinkholes I intersected a random selection of 400 USGS-recorded sinkholes from the Dunigan study with the derived depression polygons and exported the coinciding features. The resulting shapefile represented potential training sinkholes in Knox County. Dunigan considered all closed contour depressions to represent sinkholes; however, other non-sinkhole features (e.g., retention ponds and quarries) are also represented by closed contours on topographic maps. Therefore, it was important to inspect the potential training sinkholes to verify that they coincide with true sinkholes. The inspection procedures involved two parts. First, I verified that all potential training sinkholes fell within karst regions. Then, I used visual inspection of topographic maps and aerial imagery to determine if the depression appeared to be a true sinkhole (e.g., not labeled quarry and did not appear to be a non-sinkhole depression). Verified sinkholes were used as training sinkholes to identify and quantify the morphological characteristics of sinkholes in the region.

Step Three: Identify Likely Sinkholes

I then applied a two-step filtering process to identify the depressions that are most likely to represent true sinkholes. In the first step, I used the morphometric characteristics of training sinkholes to identify likely sinkholes. Threshold values were selected to separate sinkholes from other non-sinkhole depressions based on the 5^{th} and 95^{th} percentiles of the morphometric characteristics of sinkholes in the training dataset. For area, complexity, and elongation I considered the 95^{th} percentile to be a sufficient cut-off threshold to weed out depressions that are unlikely to represent true sinkholes based on visual observation of sinkholes in the region. For example, visual observation found that large depressions in the study area were more likely to represent non-sinkhole depressions, such as valleys, quarries, and other large anthropogenic features. In addition, visual inspection of sinkholes in the study area found that the true sinkholes are generally of low complexity (e.g., < 0.18) while other depressions, particularly anthropogenic features, are of higher complexity (e.g., > 0.25). Finally, visual observation found that sinkholes in the study area are generally circular or elliptical rather than elongated. Therefore, large values for elongation are more likely to represent non-sinkhole features such as culverts, ditches, valleys and dry stream beds. For depth and slope I considered the 5^{th} percentile of sinkholes in

the training dataset to be a sufficient threshold for weeding out very shallow depressions. While some very shallow depressions could represent true sinkholes, it would be very difficult to validate such locations through visual inspection of aerial imagery. Therefore, in this case, I considered only depressions with values above the 5th percentile of depth and slope to be likely sinkholes. I used additional analyses to flag areas with urban and agricultural development as these areas could yield false positives. Thus, in the second step of the process, I applied soft filters through the use of buffers and intersect analysis to flag these potential false positives. To identify potential non-sinkhole depressions that could be the result of urban development, I applied a uniform 2-meter buffer to all building footprints in the study area. I also applied buffers based on road type as follows: major arterial (34-meter buffer), minor arterial (26-meter buffer), major collector (21-meter buffer), minor collector (18 meters buffer), alleys (6 meters buffer), and walkways (1.5-meter buffer). Intersect analysis was then applied to determine if potential sinkholes intersected wetlands as classified in the USFWS wetlands mapper. The wetlands mapper includes detailed information on the wetland type, Cowardin classification, wetland description, and special modifiers. This information is important for two main reasons: 1) for identifying false positives that are farm ponds, retention ponds, or other anthropogenic water features as determined by the special modifiers description; and 2) for identifying permanently flooded natural wetlands that could serve as potential paleolimnological sampling sites for paleoflood research as determined by the wetland classification and description. An additional soft filter (soils of fluvial origin) was applied to identify sinkholes that could also record evidence of paleofloods. To flag sinkholes that intersect the building and road buffers, the wetlands, or soils of fluvial origin, I flagged sinkholes that intersected wetlands by overlaying the polygon feature and assigning a binary to flag intersecting features. To do so, I first created a new column in the attribute table and used the *select by attribute* tool to select the likely sinkholes that intersect wetlands or the defined buffers. Next, I flagged the sinkholes by using the *field calculator* tool to assign the value of one to intersecting sinkholes and zero to non-intersecting sinkholes

Step Four: Conduct an Accuracy Assessment

I performed an accuracy assessment to test the results of the method. First, I used the *create random points* tool in the data management toolbox to create 400 random points. Then I

buffered the points at 100 meters and zoomed to each location to identify 50 sinkholes and 50 non-sinkhole depressions within the buffered areas (one of each per buffered area, if possible) using visual inspection of 2-foot contours displayed over Google Earth aerial imagery. This allowed for the random identification of 100 sample points. Because the 2-foot contours were derived from the same DEMs used in my analysis, if a sinkhole appeared on the 2-foot contours, I expect it would be captured in the results. I created a contingency table to test the accuracy of the results of the method against these sample data.

Step Five: Identify likely sinkholes with the potential for the preservation of paleoflood evidence

Because I was interested in finding sinkholes in which I could study paleoflood deposits together with environmental proxies preserved in sediments, I focused the search to sinkhole ponds. Information on paleofloods collected from other locations along the river, including dry sinkholes, could also support paleoflood investigations; however, these locations are outside the scope of the work discussed here.

To identify sinkholes with the potential of having preserved paleoflood evidence, I first intersected the sinkholes that I detected with flood hazard areas as designated by FEMA. In this thesis, I focused on sinkholes within the 100- and 500-year flood zones of the Tennessee River (areas of 1-percent annual chance flood and 0.2-percent annual chance flood, respectively) (see Figure 2.4.). Then, to identify sinkhole ponds, the floodplain sinkholes were intersected with wetland shapefiles downloaded from the USFWS National Wetlands Inventory wetlands mapper. The potential for paleoflood evidence to be preserved in sediments of sinkhole ponds depends on the status of the sinkhole as a permanently flooded waterbody, the proximity of the sinkhole to the flood source, and the age of the sinkhole. For this work, I consider only sinkholes that meet the following conditions as potentially suitable paleoflood sampling locations: 1) the sinkhole is within the 100 or 500-year FEMA flood zone; 2) the sinkhole intersects a continuously flooded natural waterbody as recorded in the USFWS wetlands mapper; and 3) there is some evidence to suggest the sinkhole is old enough to preserve environmental records based on its presence on historical topographic maps. If a sinkhole that met the aforementioned criteria were found, this location would be considered as a potentially suitable sampling site for future research.

Table 2.1. List of Data Used and Their Source

Data	**Source**
LiDAR DEMs	Tennessee Department of Finance and Administration's GIS data portal: *https://www.tn.gov/finance/sts-gis/gis/data.html*
Point Locations of Recorded Sinkholes	Dunigan's Tennessee Landforms Website: *https://tnlandforms.us/landforms/sinks.php*
Shapefiles of Karst Areas	USGS Karst in the United States dataset: *https://pubs.usgs.gov/of/2014/1156/*
Two-Foot Contour Shapefiles	Tennessee Department of Finance and Administration's GIS data portal: *https://www.tn.gov/finance/sts-gis/gis/data.html*
Knox County Roads Shapefiles	U.S. Census Bureau's Topologically Integrated Geographic Encoding and Referencing (TIGER) website: *https://tigerweb.geo.census.gov/tigerweb/*
Building Footprint Shapefiles	Tennessee Department of Finance and Administration GIS data portal: *https://www.tn.gov/finance/sts-gis/gis/data.html*
Wetland Shapefiles and Classifications	USFWS Wetland Mapper: *https://www.fws.gov/wetlands/data/mapper.html*
Historical Topographic Maps	http://historicalmaps.arcgis.com/usgs/

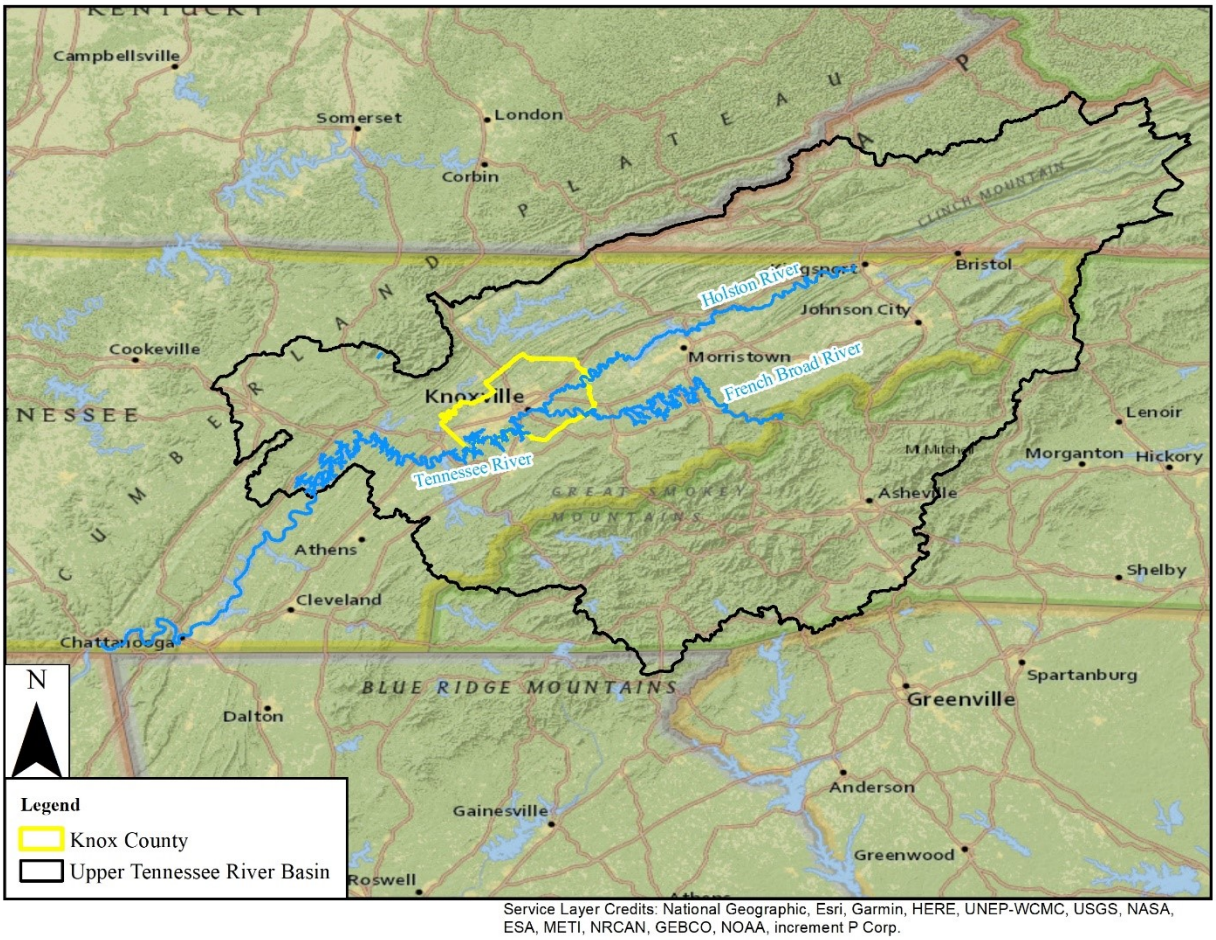


Figure 2.1. Map of Case Study Area: Knox County, Tennessee

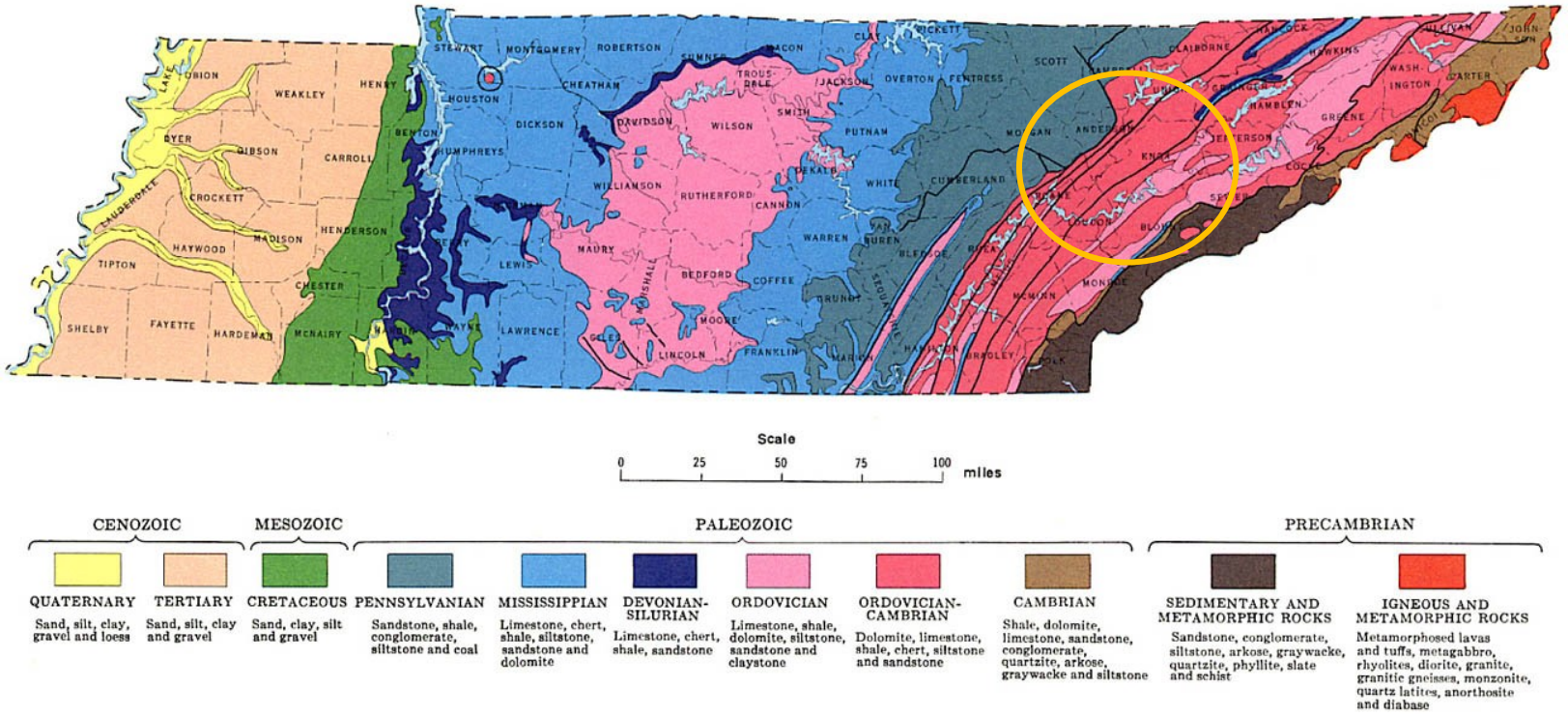


Figure 2.2. Generalized Geologic Map of Tennessee

Source: "Generalized Geologic Map of Tennessee", Tennessee Department of Environment and Conservation, https://www.tn.gov/content/dam/tn/environment/geology/images/geology_geologic-map-lg.jpg, 1 April 2020.

Within the gold circle lies Knox County, the study area of this research.

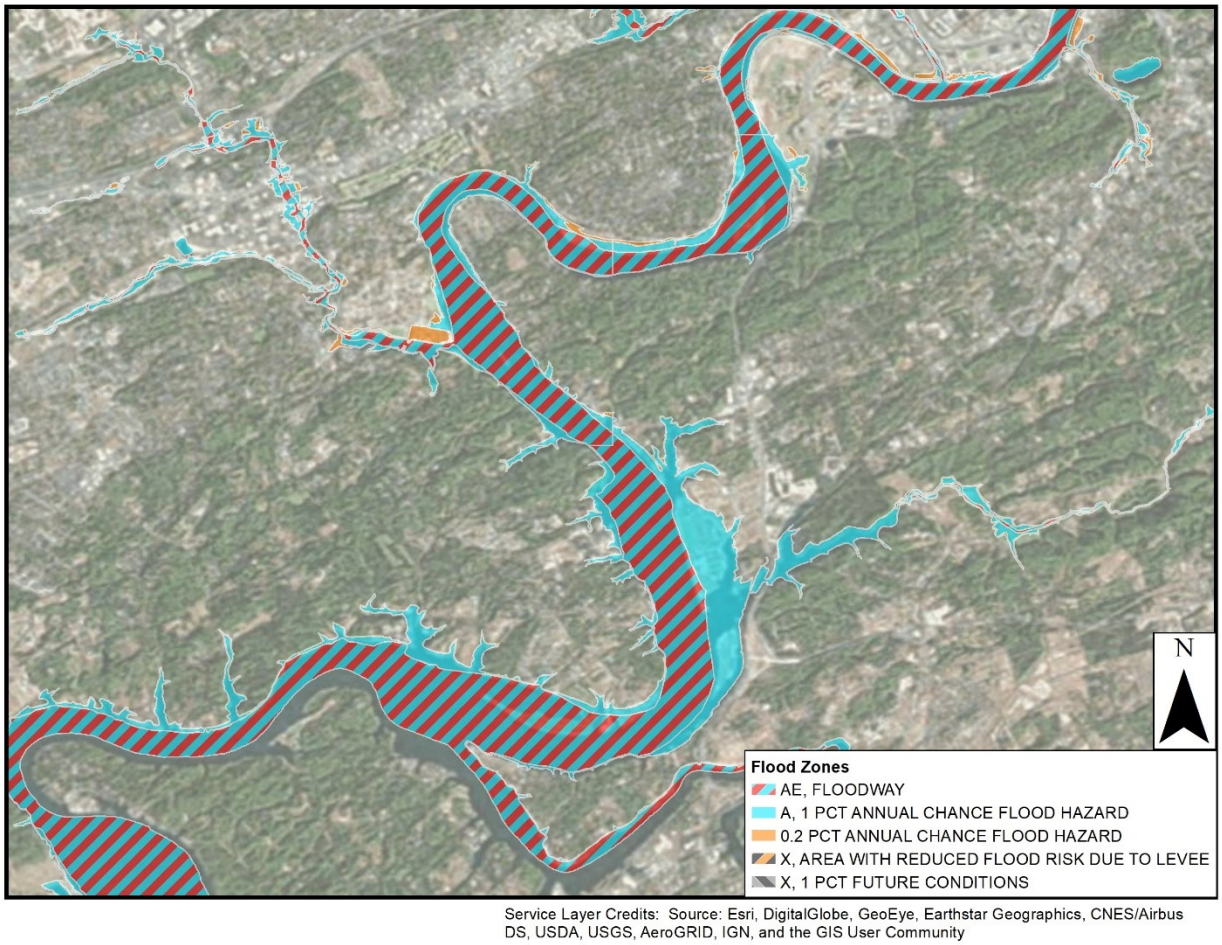


Figure 2.3. Example of FEMA Flood Hazard Extent Along the Tennessee River in Knox County, Tennessee

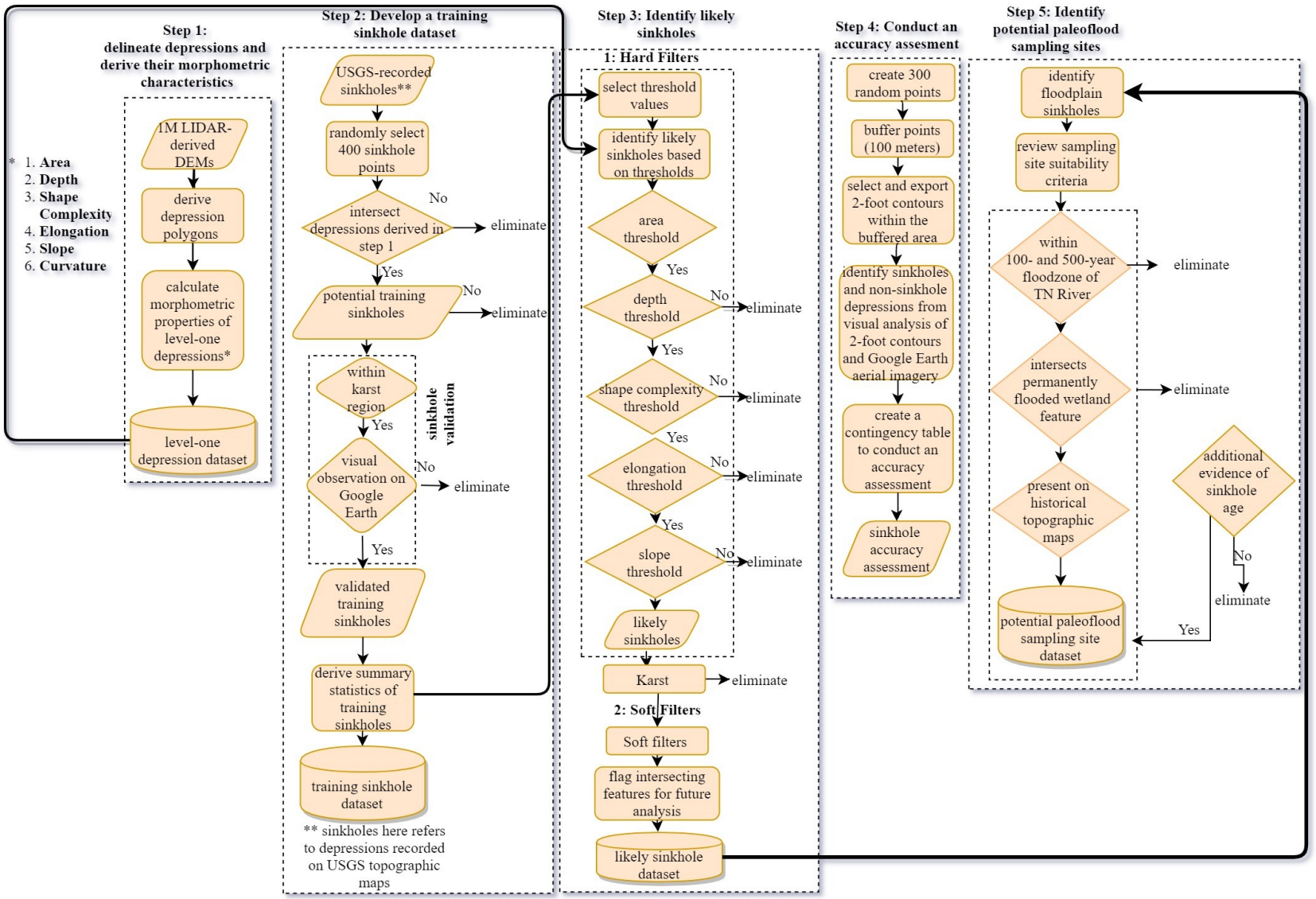


Figure 2.4. Full Method Workflow

CHAPTER THREE
RESULTS AND DISCUSSION

Results

Step One: Delineate Depressions

As a result of step one, a total of 43,937 depressions were detected in Knox County using the level-set method with the predefined parameters level-set method detected all surface depressions across the landscape including natural features such as stream beds, valleys, and karst sinkholes as well as anthropogenic features such as quarries, retention ponds, and stormwater culverts (Figure 3.1.). Detailed below are the summary statistics of the morphometric properties of the depressions including area, depth, elongation, shape complexity, and slope (Table 3.1). The largest depression detected was 132,091 square meters, approximately the size of 25 football fields, while the smallest depression detected was 46 square meters, roughly the size of a two-car garage. Depth values ranged from 0.30 meters to 32.24 meters. Elongation values ranged from 0.00 to 0.97. Features with an elongation value of or near zero are roughly square or circular, but as the elongation value for a given feature increases, the feature becomes increasingly linear (Figure 3.2.). Shape complexity values ranged from 0.02 to 0.89. Features with a shape complexity value at or near zero are simple, but as the shape complexity value for a given feature increases, the feature becomes increasingly complex (Figure 3.3.). The slope of the walls of the depressions ranged from a minimum 0.6% (nearly level) to a maximum of 65% (very steep). Most of the depressions have negative curvature values showing that they are convex; however, concave depressions, represented by positive curvature values, accounted for a small number of depressions (approximately 830 of the 43,937 sinkholes).

Step Two: Develop a Training Sinkhole Dataset

As a result of step two, I found that 206 of the 400 USGS-recorded sinkholes points randomly identified in this step coincided with the locations of depressions derived in step one. The validation procedures eliminated 30 of these 206 locations resulting in a training sinkhole dataset with 176 verified sinkholes. These sinkholes ranged from 109.7 square meters to 33,561 square meters in area and 0.30 meters to 17.86 meters in depth. The maximum elongation value

for sinkholes in the training dataset was 0.70 while the maximum complexity value was 0.23. Slope values ranged from 1.33% (very gentle slope) to 22.17% (moderately steep slope). All of the sinkholes in the training dataset had negative curvature values showing that they are convex. Table 4.2 displays complete summary statistics of the morphometric properties of depressions in the training sinkhole dataset. Overlapping density plots show the distribution and spread of the morphometric characteristics of the 43,937 depressions derived in step one and the 176 training sinkholes derived in step two (Figure 3.4.).

Step Three: Identify Likely Sinkholes

As a part of step three, I selected the following hard filters: area < 15,000 m^2; depth > 0.93 m; complexity < 0.18; elongation < 0.57; and slope > 3.30%. The area, depth, complexity, elongation, and slope filters resulted in the elimination of non-sinkhole depressions which did not meet the specified parameters to be classified as likely sinkholes. The results for each morphometric parameter are as follows: 177 depressions did not meet the area threshold; 28,433 depressions did not meet the depth threshold; 24,909 depressions did not meet the complexity threshold; 20,765 depressions did not meet the elongation threshold; and 5,962 depressions did not meet the slope threshold. After applying the aforementioned filters, I identified 7,401 potential sinkholes within the study area. Intersecting the potential sinkholes with information on karst in the region led to the elimination of 158 of the potential sinkholes resulting in a dataset of 7,248 likely sinkholes for Knox County. I found that 613 of the likely sinkholes that I identified were previously recorded as depressions identifiable on USGS topographic maps while 6,630 were not previously recorded. Applying soft filters, I identified 927 sinkholes that intersected the defined building buffers; 2,457 sinkholes that intersected the defined road buffers; 813 sinkholes that intersected NWI-recorded wetlands; and 2,019 sinkholes that intersected soils of fluvial origin.

Step Four: Conduct an Accuracy Assessment

As a result of step four, the accuracy assessment results show that the overall classification accuracy for the method is 87% while the misclassification rate is 13%. The model classified 47 true sinkholes and 53 non-sinkhole depressions. Of those 47 true sinkholes, 42 were correctly classified using the method while 5 were misclassified. Of those 53 non-sinkhole

depressions, 45 were correctly classified using the method while 5 were misclassified. Therefore, the true positive rate for the method is 84%.

Step Five: Identify likely sinkholes with the potential for the preservation of paleoflood evidence

As a result of step five, I found twelve and nine likely sinkholes that intersect the 100-year flood zone and the 500-year flood zone of the Tennessee River, respectively. Of the twelve likely sinkholes in the 100-year flood zone, I found that three intersect wetland features. None of the likely sinkholes in the 500-year flood zone intersect wetland features. The three wetlands that intersect the 100-year flood zone are classified by the USFWS as follows: PFO1A (palustrine, forested, broadleaf deciduous, temporarily flooded); PSS1A (palustrine, scrub-shrub, broadleaf deciduous, temporarily flooded); and L1UBHh (lacustrine, limnetic, unconsolidated bottom, permanently flooded, diked/impounded). I did not perform any additional analysis on the temporarily flooded features. Using historical topographic maps dating back to 1886 for Knox County, I searched for the permanently flooded wetland feature that I identified (located at 35.95016187,-83.95090893) in the 100-year flood zone of the Tennessee River; however, I was not able to identify it even on the most recent topographic map of 1983. Through analysis of aerial imagery, I determined that this location is likely to be a residential decorative pond rather than a sinkhole pond. Therefore, I was unable to identify a sinkhole on the floodplain suitable for paleolimnological research in Knox County based on the method described above.

Discussion

Many existing sinkhole datasets rely primarily on traditional methods of sinkhole detection (e.g., field observations, visual observation of topographic maps, and aerial imagery interpretation). However, these methods provide inventories with several weaknesses. For example, while sinkhole inventories developed solely from field observation have the ability to provide detailed information on sinkhole status and characteristics, producing these inventories is time intensive. Therefore, field observation typically results in sinkhole inventories that are relegated to small study areas. In addition, although topographic map interpretation is used to produce sinkhole inventories covering large study areas, without additional filtering this analysis results in the inclusion of many non-sinkhole depressions. Next, while aerial imagery can be a

useful tool for researchers looking to identify sinkholes, the reliability of this technology largely depends on the resolution of the photographs as well as the experience of the observers. Therefore, visual analysis of aerial imagery is vulnerable to the observer's subjective analysis. Furthermore, such inventories are often misrepresentative and incomplete as the rate of sinkhole formation and sinkhole filling outstrip the production of updated topographic maps. Another weakness of topographic map interpretation is that the inventories developed using this method are bound by the often-coarse resolution of the maps (for example, the USGS 1:24,000 scale topographic maps that are widely used). With such analyses, small and shallow depressions can easily be missed.

The proposed method builds on both the level-set method and other existing sinkhole detection methods to develop a method that offers several strengths in terms of sinkhole detection. Compared with traditional methods of sinkhole detection, the proposed method is better in several respects. First, by incorporating the level-set method of depression detection, the proposed method is able to take advantage of several strengths of level-set. For example, the proposed method is able to efficiently identify and delineate sinkholes (even small and shallow sinkholes) from high-resolution LiDAR DEMs. In addition, because level-set is an automated approach to depression delineation, the proposed method can be applied across comparatively large study areas and inventories can be regularly updated with relative ease as new DEMs are generated. Finally, whereas many existing inventories simply mark sinkhole locations with a point, the application of level-set allows for the delineation of sinkhole boundaries. Second, the use of the multiple-step filtering process is able to constrain the depression results to those locations that are most likely to represent true sinkholes based on the characteristics of verified sinkholes in the region. These filters allow for a relatively objective approach to sinkhole detection as the determination of true and false sinkholes is based on the characteristics of verified sinkholes rather than the analyst's subjective judgment. Another strength of this method is the use of soft filters to identify sinkholes of interest based on their proximity to anthropogenic features. This proximity is important for two distinct reasons. The first reason is that sinkholes close to anthropogenic features could be anthropogenic non-sinkhole depressions such as stormwater culverts and retention ponds. Therefore, these sinkholes require additional analysis to confirm that they are in fact true sinkholes. In addition, proximity to anthropogenic features is

important due to the fact that sinkhole development and collapse can cause costly damage to these sites. Thus, the use of soft filters can allow researchers to identify sinkholes within close proximity of anthropogenic features that may need to be monitored to protect property and human lives. This is a potentially valuable application of the method.

The proposed method also allows for the development of more detailed sinkhole inventories when compared to sinkhole inventories generated from traditional methods. For example, recorded in the results are not only the locations of likely sinkholes, but also relevant information such as sinkhole size, depth, curvature, and slope. These characteristics can be used to provide insight into sinkholes in the region beyond what is typically recorded in sinkhole inventories that are developed from traditional detection methods.

Along with the ability to improve sinkhole detection and inventories, this method also offers potential for identifying promising sampling sites for paleoflood research. While evidence in slackwater deposits on broad overbank areas may be lost due to erosion from subsequent flood events or biological activity sinkholes can trap and maintain flood evidence. Thus, analysis of sediment cores collected from sinkholes can allow for a more detailed reconstruction of long-term flood histories in comparison to analysis of slackwater deposits collected from broad overbank areas. Sinkholes located within floodplains are of particular interest as they are able to collect sediments from flood events. Therefore, to extend the method to identify potential paleoflood sampling sites this work focused on floodplain sinkholes as potential recorders of paleofloods.

The case study conducted in Knox County, Tennessee demonstrates the usefulness of this method in identifying and characterizing sinkholes. While various researchers and agencies (including USGS, ORNL, and TDOT) have conducted studies of sinkholes in Knox County, these studies primarily relied on traditional methods of sinkhole detection; therefore, the resulting sinkhole inventories were typically inaccurate and incomplete based on the aforementioned shortcomings of traditional methods. However, using the method discussed here I was able to develop an enhanced and updated sinkhole inventory for the county, locating 7,248 depressions compared to the 1,663 sinkholes that were previously identified based on topographic maps.

Very little information on the characteristics of sinkholes was recorded within the case study area of Knox County. Therefore, I developed a set of training sinkholes based on their presence on topographic maps, coincidence with level-one depressions, and their appearance on aerial imagery. For this study, I considered the aforementioned criteria as sufficient for identifying training sinkholes. In the future, field work should be carried out to verify that the training sinkholes do in fact represent true sinkholes. If the method discussed in this thesis were to be applied in a region where more detailed information on verified sinkholes already exists, such information should be used in lieu of the training data developed as described in step two of this method. In addition, because Knox County lacked detailed information on the characteristics of sinkholes, I set broad parameters for the level-set method in order to identify as many potential sinkholes as possible. However, for regions with more detailed data, this information should be used in order to calibrate the level-set method parameters based on the characteristics of known sinkholes in the region.

Soft filters were used to identify sinkholes of particular interest based on their coincidence with man-made structures; however, detailed review of these sinkholes has not been carried out at this point. Therefore, in the next phase of this research, analyses of aerial imagery and field reconnaissance should be conducted in order to review sinkholes of interest to classify these locations as either anthropogenic features that were misclassified by the method or as potentially dangerous sinkholes due to their proximity to vulnerable infrastructure. For non-sinkhole depressions misclassified by the method, review of the morphometric characteristics of these depressions could potentially allow for the adjustment of the hard filters to eliminate the inclusion of anthropogenic non-sinkhole depressions. In addition, while sinkholes were flagged based on their coincidence with wetlands and soils of fluvial origin, the information on soils of fluvial origin was not used in the identification of potential paleoflood samplings sites. Therefore, in the future, this information should be used to aid in the investigation of potential paleoflood sampling sites.

Although this thesis only applied four soft filters (e.g., intersection with buffers applied to shapefiles of building and roads, wetlands, and fluvial soils) other information could be used in this capacity to improve automated sinkhole detection. One such option for improved sinkhole identification involves the use of data derived from landform classification methods (such as the

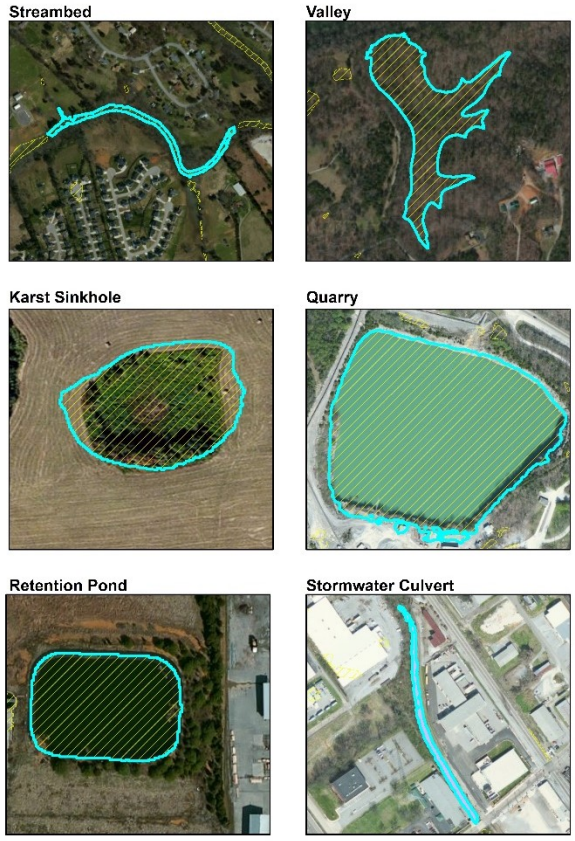
geomorphon method) (Jasiewicz and Stepinski 2013). Landform classification has the potential to improve the identification of sinkholes from the larger class of depressions by looking at the relationship between landform characteristics surrounding and within sinkholes compared to landform characteristics surrounding and within both natural and anthropogenic non-sinkhole depressions. The use of landform classification as discussed here has not been applied, however, it is possible that non-sinkhole depressions and sinkholes have distinct landform characteristics. If so, then the use of landform classification data could serve as a powerful tool for separating sinkholes from other non-sinkhole depressions.

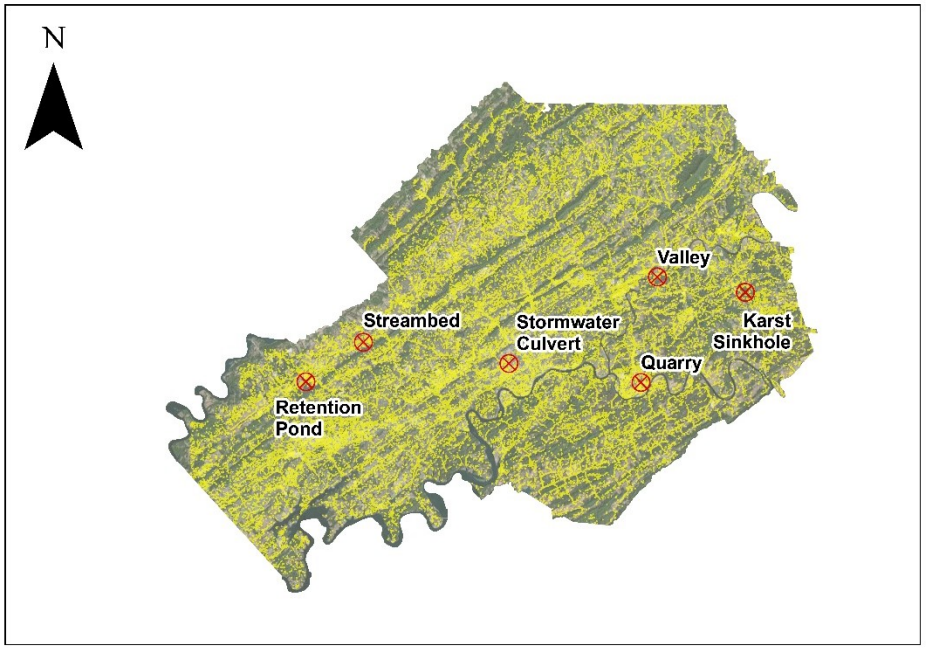
To conduct the accuracy assessment, data of true sinkholes in the case study area should be used. Because the region lacked an up-to-date sinkhole dataset, I developed training data that relied on the analysis of aerial imagery and 2-foot contours. When relying on visual analysis of aerial imagery alone, sinkholes that are small, shallow, or that are under dense canopy cover are often missed. However, the use of 2-foot contours provides for the identification of sinkholes that would otherwise not have been identified as these contour maps allow the analyst to visualize terrain elements at a finer detail. The 2-foot contours are derived from the same LiDAR data used in the delineation of depressions in the region; therefore, sinkholes present on these 2-foot contours should also be recorded in the inventory developed by the proposed method. For regions with more detailed, up-to-date sinkhole inventories, this information could be used to test the accuracy of the method in this thesis in lieu of the method discussed here for deriving sample data. However, for best results, the accuracy assessment data should be developed from aerial imagery and contours that rely on the same LiDAR data used for delineating sinkholes or the accuracy assessment may not account for the dynamic nature of sinkholes.

While this case study demonstrates the usefulness of this method in identifying and characterizing sinkholes, I was unable to identify any potential paleoflood sampling sites in the case study area based on the criteria outlined in this thesis. I attribute this finding to two main factors: 1) focusing only on water-filled sinkholes and 2) focusing only on sinkholes within the 100- and 500-year flood zones of the Tennessee River. First, I limited potential sampling sites to sinkhole ponds as I was interested in identifying sinkholes in which I could study paleoflood deposits together with environmental proxies preserved in sediments. However, because LiDAR is typically unable to penetrate water, it is possible that very few water-filled sinkholes were

identified by the level-set method. In addition, those that were identified might have been eliminated from the sinkhole dataset based on the slope threshold due to the fact that the presence of water would make the sinkhole appear flat. Therefore, extending the search in the future to include dry sinkholes (focusing on those in the historic floodplains of the Tennessee River with soils of fluvial origin) could allow for the identification of more paleoflood sampling sites. Another approach would be to eliminate the slope threshold which could be useful in identifying more water-filled sinkholes.

The second factor contributing to why I was unable to identify a potential paleoflood sampling site within the case study area was the fact that I only considered sinkholes within the 100- and 500-year flood zones as suitable sites. For the Tennessee River, the 100- and 500-year flood zones represent a small area along the river with flood waters from large and rare floods likely to extend beyond this area (see Figure 2.4. for an example of flood zone extent along river). An improvement to the method would be to use information from historical flood events (e.g., the 1867 megaflood) to model the historical flood zones of the Tennessee River using the Hazus-MH software that is developed by FEMA. The modeled flood zone could then be used as the parameter for identifying sinkholes that are likely recorders of flood evidence rather than considering only those sinkholes found within the 100- and 500-year flood zones Because more detailed flood modeling along the entire Tennessee River would be time-intensive, preliminary analysis of sinkhole locations along the river would be useful to identify regions with a high density of sinkholes. This approach would allow analysts to focus their efforts on promising locations.





Depression	Area (square meters)	Depth (meters)	Elongation	Complexity	Slope (%)	Curvature (meters)
Streambed	7926.40	1.10	0.69	0.86	3.42	-2.18
Valley	38612.40	13.22	0.35	0.50	16.72	-0.52
Karst Sinkhole	3925.75	5.18	0.21	0.03	12.25	-0.25
Quarry	74679.2	12.68	0.16	0.05	43.46	-11.3
Retention Pond	4080.78	1.12	0.3	0.02	16.66	0.2
Stormwater Culvert	2033.42	1.07	0.88	0.71	10.02	-5.58

Figure 3.1. Depressions in Knox County, Tennessee

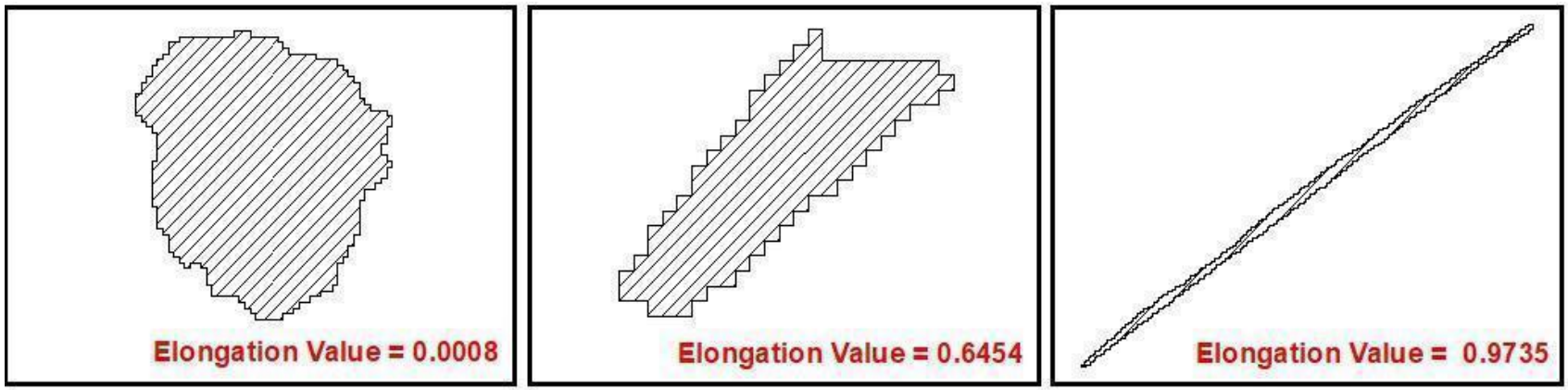


Figure 3.2. Examples of Elongation Values

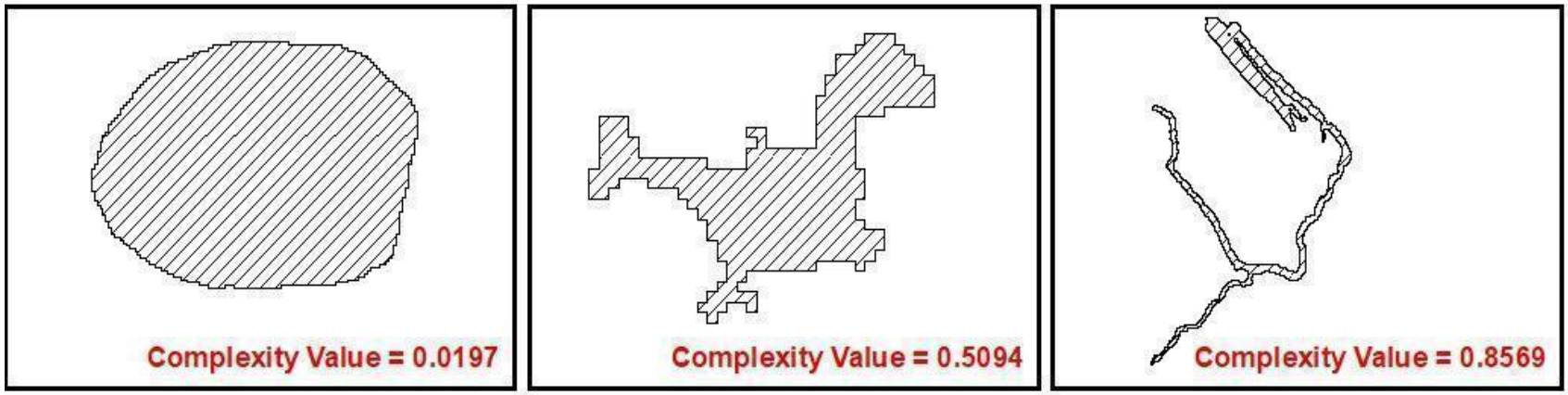


Figure 3.3. Examples of Complexity Values

Table 3.1. Summary Statistics of Depressions

Statistic	Area(m^2)	Depth (m)	Elongation	Complexity	Slope (%)	Curvature (m)
Minimum	46.45	0.30	0.00	0.02	0.07	-91.24
5^{th} Percentile	52.84	0.33	0.08	0.06	2.31	-9.47
Median	245.03	0.69	0.55	0.2	7.4	-1.73
Mean	848.27	1.04	0.52	0.24	8.91	-2.9
95^{th} Percentile	3,333.14	2.85	0.86	0.54	18.92	-0.69
Max	132,091.81	32.24	0.97	0.89	65.52	-0.18

Table 3.2. Summary Statistics of Training Sinkhole Depressions

Statistic	Area(m^2)	Depth (m)	Elongation	Complexity	Slope (%)	Curvature (m)
Minimum	109.70	0.30	0.00	0.02	1.33	-7.86
5^{th} Percentile	1,000.00	**0.93**	0.036	0.03	**3.30**	-0.99
Median	3,723.10	3.44	0.28	0.08	8.32	-0.40
Mean	5,080.60	4.09	0.28	0.08	8.89	-0.52
95^{th} Percentile	**14,763.08**	8.43	**0.57**	**0.18**	16.33	-0.11
Max	33,556.10	17.86	0.71	0.23	22.17	-0.05

***Bolded values were used to determine hard filters for step three**

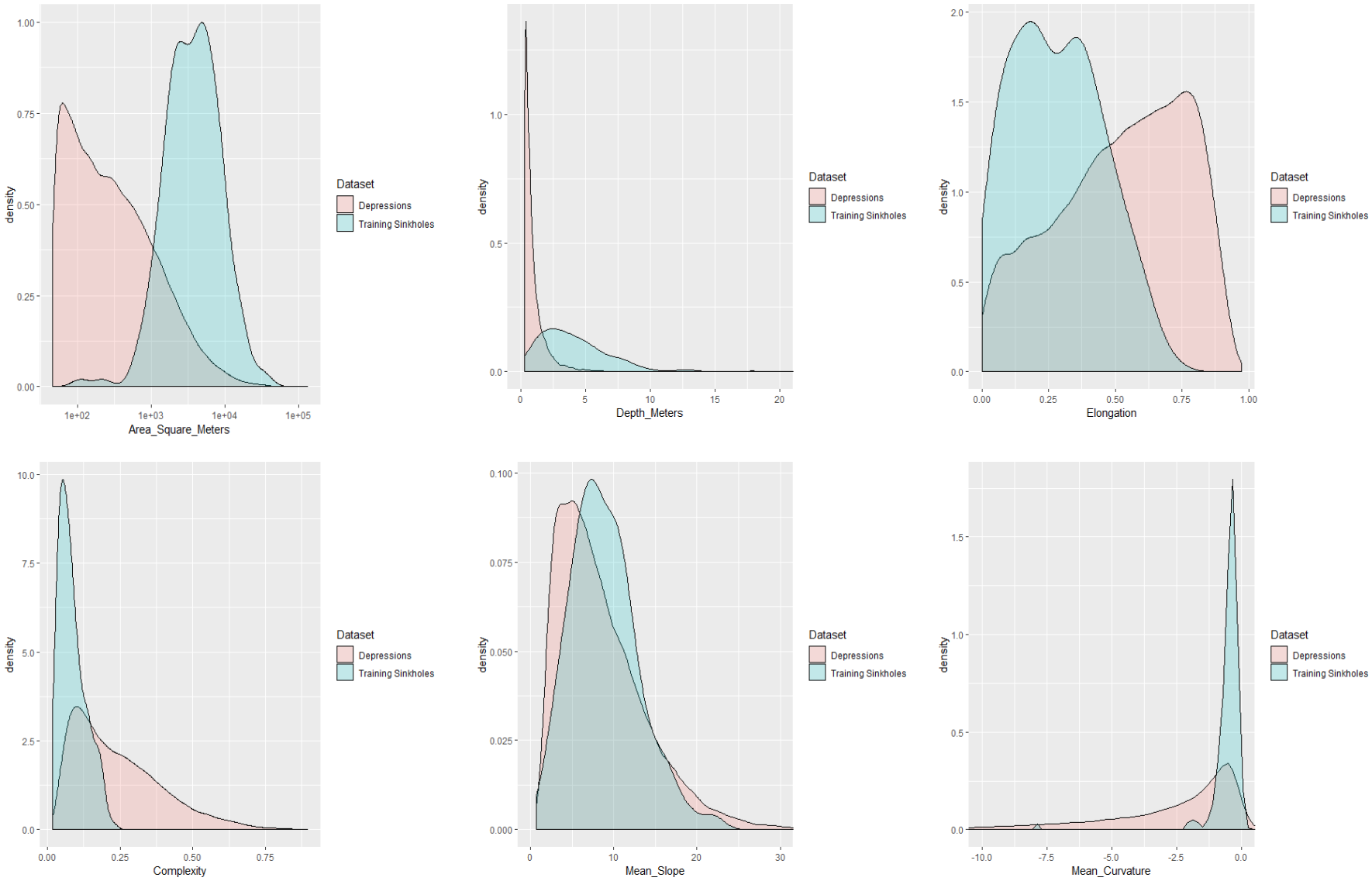


Figure 3.4. Overlapping Density Plots of Depressions and Training Sinkholes

Table 3.3. Accuracy Assessment for Identified Sinkholes

		Model Prediction		
		True Sinkhole	*Non-Sinkhole Depression*	*Total*
Actual	*True Sinkhole*	*42*	*8*	*50*
	Non-Sinkhole Depression	*5*	45	*50*
	Total	*47*	*53*	*100*

CHAPTER FOUR
CONCLUSIONS

Many existing sinkhole inventories are based on traditional methods of sinkhole detection that rely on outdated topographic maps, aerial imagery, and field observations that cover relatively small or disjunct study areas. With the development of modern remote-sensing technology, high-resolution remotely sensed data can be used to provide more detailed mapping and analyses of landscape features including sinkholes. Using this high-resolution data, updated methods of sinkhole detection and characterization can produce enhanced inventories that can serve many purposes, such as use in flood-hazard mapping, land-use planning, sinkhole-hazard mapping, and paleoenvironmental reconstructions. In this thesis I present a method for detecting and characterizing sinkholes and for identifying particular sinkholes with the potential of having preserved paleoflood evidence.

The proposed method builds on both the level-set method and other existing sinkhole detection methods to develop a method with several strengths. For example, the proposed method uses high-resolution DEMs to efficiently identify and delineate sinkholes, recording even small and shallow depressions. Because level-set is an automated approach to depression delineation, the proposed method can be applied across comparatively large study areas and inventories can be regularly updated with relative ease as new DEMs are generated. Another strength of the proposed method is the application of filters that allow for a more objective approach to sinkhole detection as the determination of true and false sinkholes is based on the characteristics of verified sinkholes rather than an analyst's subjective judgment. Not only can filters be used to identify likely sinkholes, but they also can be used to flag sinkholes of interest based on their proximity to anthropogenic structures. Furthermore, this method allows for the development of more detailed records of sinkholes. For example, recorded in the results are not only the locations of likely sinkholes, but also relevant information such as sinkhole boundary, size, depth, curvature, and slope. These characteristics can be used to provide useful insight into sinkholes in the region beyond what is typically recorded in sinkhole inventories that are developed from traditional detection methods. Finally, I found that the method presented in this thesis can be extended to identify sinkholes that can serve as superior paleoflood recorders due to their ability to receive, trap, and maintain evidence from past flood events.

With respect to identifying potential paleoflood sampling sites within floodplain sinkholes, adjustments should be made in the future to extend the search criteria to allow for the identification of additional potential sampling sites. For example, in this work, I considered only sinkhole wetlands within the 100- and 500-year flood zones of the Tennessee River as potential sampling sites. However, more detailed information on flood histories including soil origins and flood modeling based on information from historic flood events could be used to identify sinkholes outside of these zones that have the potential for maintaining flood evidence. In addition, although sinkhole wetlands offer an advantage for studying paleoflood deposits together with environmental proxies preserved in sediments, dry sinkholes also offer the potential for trapping and preserving flood evidence. Therefore, dry sinkholes can be considered as suitable sites for paleoflood investigations in the absence of a sinkhole wetland.

This research is particularly important in this region because the Tennessee River is home to several nuclear power plants that are vulnerable to flooding; therefore, paleoflood studies conducted in this region can help researchers understand the potential flood risk for these vulnerable sites. Furthermore, since sinkholes offer an advantage for reconstructing long-term flood histories in comparison to slackwater deposits collected from broad overbank areas, this method could be particularly valuable in the southeastern United States where the presence of a humid climate and wetter soils are more likely to lead to erosion or bioturbation of evidence of past flood events.

LIST OF REFERENCES

Angel, J. C., Nelson, D. O., & Panno, S. V. (2004). Comparison of a New GIS-Based Technique and a Manual Method for Determining Sinkhole Density: An Example From Illinois' Sinkhole Plain. *Journal of Cave and Karst Studies*, *66*(1), 9–17. https://doi.org/EffondrementVD

Bauer, T. (2010). Evaluation of Paleoflood Peak Discharge Estimates in Hydrologic Hazard Studies. *Reclemation: Managing Water in the West*, *Report DSO*(October 2010), 3–15.

Benito, G., & Diez-Herrero, A. (2015). *Chapter 3 - Palaeoflood Hydrology: Reconstructing Rare Events and Extreme Flood Discharges*. Elsevier.

Benito, G., & Thorndycraft, V. (Eds.). (2004). *Systematic, Palaeoflood and Historical Data for the Improvement of Flood Rrisk Estimation: Methodological Guidelines* (1st ed.). Madrid: CSIC - Centro de Ciencias Medioambientales. Retrieved from http://www.ccma.csic.es/dpts/suelos/hidro/sphere/index.html

Bondesan, A., Meneghel, M., & Sauro, U. (1992). Morphometric Analysis of Dolines. *Internation Journal of Speleology*, *21*.

Crownover, S. H., Collins, M. E., & Lietzke, D. A. (1994). Soil-stratigraphic correlation of a doline in the Valley and Ridge Province. *Soil Science Society of America Journal*, (58), 1730–1738.

Davis, L. (2017). To Aid Utilities, Researchers Seek Ancient Floods Near Tennessee River – University of Alabama News. Tuscaloosa: University of Alabama.

Denton, R., Hogan, A., & Thomas, R. (2016). The Integration of Data Review, Remote Sensing and Ground Survey for a Regional-Level Karst Assessment. *Environmental & Engineering Geoscience*, *22*(1), 81–92. https://doi.org/10.2113/gseegeosci.22.1.81

Dunigan, T. (2019). Tennessee Landforms. Retrieved from http://tnlandforms.us/landforms

Galloway, D., Jones, D., & Ingebritsen, S. (Eds.). (2000). *Land Subsidence in the United States*. USGS Fact Sheet.

George, S. S. (2010). Tree Rings as Paleoflood and Paleostage Indicators. In M. Stoffel, M. Bollschweiler, D. Butler, & B. Luckman (Eds.), *Tree Rings and Natural Hazards: A State-of-the-Art, Advances in Global Change Research* (pp. 223–239). Springer. https://doi.org/10.1007/978-90-481-8736-2

Gutiérrez, F., Galve, J. P., Lucha, P., Castañeda, C., Bonachea, J., & Guerrero, J. (2011). Integrating Geomorphological Mapping, Trenching, InSAR and GPR for the Identification and Characterization of Sinkholes: A Review and Application in the Mantled Evaporite Karst of the Ebro Valley (NE Spain). *Geomorphology*, *134*(1–2), 144–156. https://doi.org/10.1016/j.geomorph.2011.01.018

Gutiérrez, F., Zarroca, M., Castañeda, C., Carbonel, D., Guerrero, J., Linares, R., … Lucha, P. (2017). Paleoflood Records from Sinkholes Using an Example from the Ebro River Floodplain, Northeastern Spain. *Quaternary Research*, *88*(01), 71–88. https://doi.org/10.1017/qua.2017.23

Hampson, P. S., Treece, M. W., Johnson, G., Ahlstedt, S. L., & Connell, J. F. (2000). Water Quality in the Upper Tennessee River Basin, Tennessee, North Carolina, Virginia, and Georgia 1994–1998. Retrieved from https://pubs.usgs.gov/circ/circ1205/pdf/circular1205.pdf

Harden, T. M., & O'Conner, J. E. (2017). *Prehistoric Floods on the Tennessee River — Assessing the Use of Stratigraphic Records of Past Floods for Improved Flood Frequency Analysis Scientific Investigations Report 2017 – 5052*. *Scientific Investigations Report 2017-5052*.

Harris, L. D. (1973). Areas with Abundant Sinkholes in Knox County.

House, P. K. (1991). *Paleoflood Hydrology of the Principal Canyons of the Southern Tortolita Mountains, Southeastern Arizona*.

Jennings, J. (1971). *An Introduction to Systematic Geomorphology: Karst* (Volume 7). Australian National University Press.

Jones, W. K., & White, W. B. (2012). Encyclopedia of Caves. In W. White & D. Culver (Eds.) (2nd ed., pp. 430–438). Elsevier. Retrieved from https://doi.org/10.1016/B978-0-12-383832-2.00061-X

Ju, E., Young, S., Chul, B., & Chang, C. (2016). Early Sinkhole Detection Using a Drone-Based Thermal Camera and Image Processing. *Infrared Physics and Technology*, *78*, 223–232. https://doi.org/10.1016/j.infrared.2016.08.009

Kemmerley, P. R. (1980). *Sinkhole Collapse in Montgomery County, Tennessee: An Overview for the Planning Process*. Nashville, Tennessee.

Ketelle, R. H., Newton, J. G., & Lamoreaux, P. E. (1987). Inventory of Karst Subsidence in the Valley and Ridge Province of East Tennessee (pp. 25–29).

Kohl, M. S. (2001). *Subsidence and Sinkholes: A Field Guide to Holes in the Ground*. *State of Tennessee Department of Environment & Conservation Division of Geology*. Nashville, Tennessee.

Kuniansky, E., Weary, D., & Kaufmann, J. (2015). The Current Status of Mapping Karst Areas and Availability of Public Sinkhole-Risk Resources in Karst Terrains of the United States. *Journal of Hydrology*. https://doi.org/10.1007/s10040-015-1333-3

Launspach, J. (2013). *Automated Sinkhole Extraction and Morphological Analysis in Northeast Iowa using High-Resolution LiDAR data*. University of Northern Iowa.

Lindsay, J. B. (2016). Whitebox GAT: A Case Study in Geomorphometric Analysis, *95*, 75–84. https://doi.org/doi:[10.1016/j.cageo.2016.07.003](http://dx.doi.org/10.1016/j.cageo.2016.07.003)

Luther, E. T. (2017). Geologic Zones. In *Tennessee Encyclopedia*. Tennessee Historical Society. Retrieved from http://tennesseeencyclopedia.net/entries/geologic-zones/

Miller, R. A., & Sitterly, P. (1977). Geologic Hazards Map of Tennessee. Tennessee Division of Geology. State of Tennessee, Dept. of Geology, Division of Geology, 1977.

Moore, H. (2013). Mapping Surface And Subsurface Karst Geohazards For Highway Projects: Sr 71 South Knoxville Boulevard Extension Knox County, Tennessee (Vol. 13th Sinkh, pp. 421–432).

Moore, H., & Drumm, E. (2018). Karst Geology in Tennessee. Knoxville: University of Tennessee Institute of Agriculture. Retrieved from https://extension.tennessee.edu/publications/Documents/W453-C.pdf

National Park Service. (2019). Valley and Ridge Province. Retrieved from https://www.nps.gov/articles/valleyandridgeprovince.htm

Newton, J. G., & Tanner, M. J. (1987). *Evaluation of Sinkhole Occurrence in the Valley and Ridge Province East Tennessee Phase III*.

Oliva, F., Viau, A. E., Bjornson, J., Desrochers, N., Bonneau, M.-A., & Trenhaile, A. (2016). A 1300 year Reconstruction of Paleofloods Using Oxbow Lake Sediments in Temperate Southwestern Quebec, Canada. *Canadian Journal of Earth Sciences*, *53*(4), 378–386. https://doi.org/10.1139/cjes-2015-0191

Pickup, G., Marks, A., & Bourke, M. C. (2002). Paleoflood Reconstruction on Floodplains Using Geophysical Survey Data And Hydraulic Modeling. In *Ancient Floods, Modern Hazards: Principles and Applications of Paleoflood Hydrology*. https://doi.org/10.1029/WS005p0047

Rodgers, J. (1953). *Geologic Map of East Tennessee With Explanatory Text*. Nashville, Tennessee.

Shofner, G., Mills, H., & Duke, J. (2001). A Simple Map Index of Karstification And Its Relationship To Sinkhole And Cave Distribution In Tennessee. *Journal of Cave and Karst Studies*, *63(2)*(January 2001), 67–75.

Stewart, J., & LaMarche, C. V. (1967). Erosion and Deposition Produced by the Flood of December 1964 on Coffee Creek Trinity County, California.

Swingle, G. D. An Introduction to the Geology of the Southern Appalachians, In ACA-MSA Fieldtrip Guidebook § (1965).

Tennessee Department of Environment and Conservation. (n.d.). Generalized Geologic Map of Tennessee. Retrieved from https://www.tn.gov/content/dam/tn/environment/geology/images/geology_geologic-map-lg.jpg

Tennessee Valley Authority. (1958). *Floods on the Tennessee River in the Vicinity of Knoxville, Tennessee*. Knoxville.

Tennessee Valley Authority. (1961). TVA Flood Control. Knoxville.

Tennessee Valley Authority. (2019). Navigation on the Tennessee River. Tennessee Valley Authority. Retrieved from https://www.tva.gov/Environment/Managing-the-River/Navigation-on-the-Tennessee-River

Theilen-Willige, B., Malek, H., Charif, A., El Bchari, F., & Chaïbi, M. (2014). Remote Sensing and GIS Contribution to the Investigation of Karst Landscapes in NW-Morocco. *Geosciences*, *4*(2), 50–72. https://doi.org/10.3390/geosciences4020050

Thornbush, M. J. (2017). Part 1: Contemporary Challenges and Current Solutions in Sinkhole Occurrence and Mitigation. *Journal of Geology & Geophysics*, *6*(June). https://doi.org/10.4172/2381-8719.1000287

Thorndycraft, V., Hu, Y., Oldfield, F., Crooks, P. R. J., & Appleby, P. G. (1998). Individual Flood Events Detected in the Recent Sediments of the Petit Lac d'Annecy, Eastern France. *Holocene*, *8*(6), 741–746. https://doi.org/10.1191/095968398668590504

Tongwen, Z., Yujiang, Y., Feng, C., & Shulong, Y. U. (2018). Reconstruction of hydrological changes based on tree-ring data of the Haba River , northwestern China, *10*, 53–67.

Turnage, K. M., Lee, S. Y., Kim, K. H., & Larse, I. L. (1997). Comparison of Soil Erosion and Deposition Rates using Radiocesium, RUSLE, and Buried Soils in Dolines in East Tennessee. *Environmental Geology*, *29*(January), 1–10.

US Geological Survey. (1993). Topographic Map Symbols, 1–4. Retrieved from https://pubs.usgs.gov/gip/TopographicMapSymbols/topomapsymbols.pdf

Waltham, T., Bell, F., & Culshaw, M. (2005). *Sinkholes and Subsidence Karst and Cavernous Rocks in Engineering and Construction*. Chichester, UK: Springer. Retrieved from https://books.google.com/books?hl=en&lr=&id=pMq80UItts8C&oi=fnd&pg=PA1&dq=sinkhole+karst&ots=rDFLUAUvgM&sig=uipG70Knjq8tbesqtmmTc3HcOIA#v=onepage&q=sinkhole karst&f=true

Wang, L., & Leigh, D. S. (2012). Late-Holocene Paleofloods in the Upper Little Tennessee River valley, Southern Blue Ridge Mountains, USA. *The Holocene*, (22(9)), 1061–1066. https://doi.org/10.1177/0959683612437863

Wiklund, J. A., Bozinovski, N., Hall, R., & Wolfe, B. (2010). Epiphytic Diatoms as Flood Indicators. *Journal of Paleolimnology*, *44*, 25–42. https://doi.org/10.1007/s10933-009-9383-y

Wilhelm, B., Arnaud, F., Sabatier, P., Magand, O., Chapron, E., Courp, T., Delannoy, J. J. (2013). Palaeoflood Activity and Clmate Change Over the Last 1400 years Recorded by Lake Sediments in the North-West European Alps, *28*, 189–199. https://doi.org/10.1002/jqs.2609

Wu, Q., Deng, C., & Chen, Z. (2016). Automated delineation of karst sinkholes from LiDAR-derived digital elevation models. *Geomorphology*, *266*(August), 1–10. https://doi.org/10.1016/j.geomorph.2016.05.006

Wu, Q., Lane, C. R., Wang, L., Vanderhoof, M. K., Christensen, J. R., & Liu, H. (2018). Efficient Delineation of Nested Depression Hierarchy in Digital Elevation Models for Hydrological Analysis Using Level-Set Method. https://doi.org/10.1111/1752-1688.12689

Zhu, J., Taylor, T. P., Currens, J. C., & Crawford, M. M. (2015). Improved Karst Sinkhole Mapping in Kentucky Using Lidar Techniques : A Pilot Study in Floyds. *Journal of Cave and Karst Studies*, *76*(December 2014), 207–216. https://doi.org/10.4311/2013ES0135

VITA

Bridgette Ingram Fritz was born in Knoxville, Tennessee to Daniel and Antoinette Fritz. She graduated from South Doyle High School in 2012 and then attended the University of Tennessee, Knoxville. During her time as an undergraduate, she served as a research assistant for Dr. Liem Tran in an investigation of paleoflood histories within the Tennessee River Basin. In 2017, Bridgette completed her Bachelor of Science in Geology and Environmental Studies, graduating *summa cum laude* and being recognized as the top graduate in Geology and Environmental Studies. She then began her Master of Science in Geography at the University of Tennessee.